Supplemental materials for

Activation of sympathetic signaling in macrophages blocks systemic inflammation and protects against renal ischemia/reperfusion injury

Table of Contents

Supplemental Figure 1

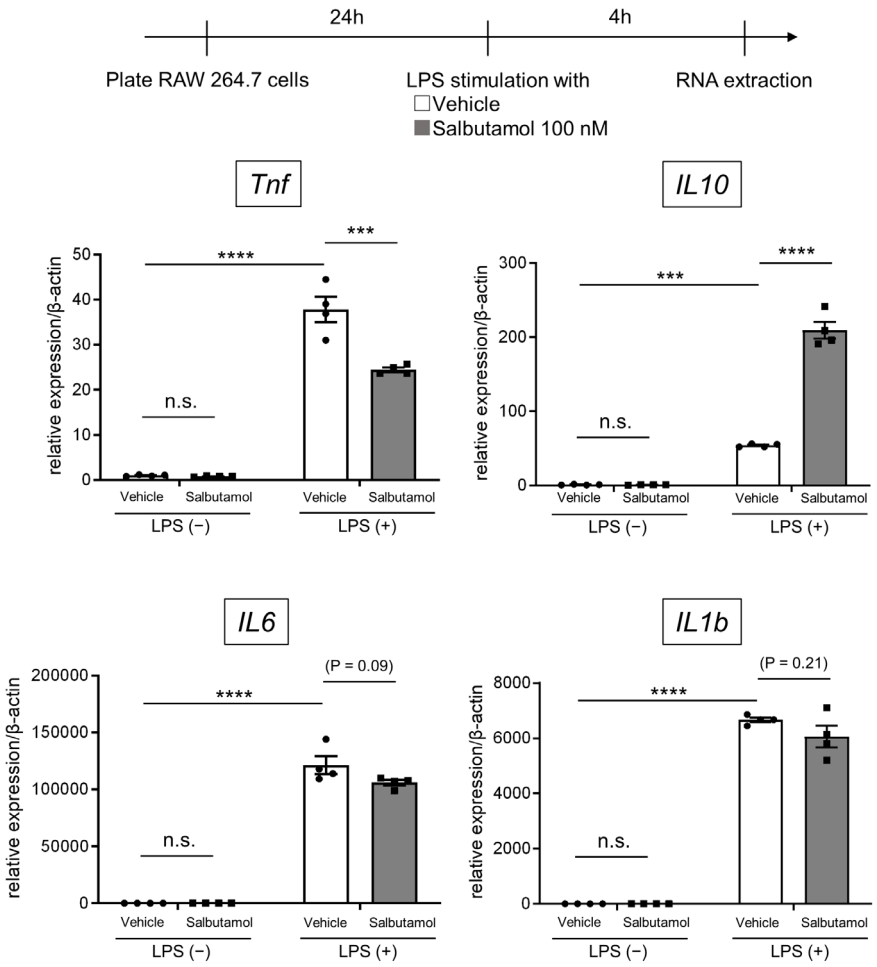

Supplemental Figure 1. The effect of β2-adrenergic receptor signaling on various inflammatory cytokines

The expressions of pro-inflammatory cytokines such as tumor necrosis factor (*Tnf*), interleukin 6 (*IL6*) and interleukin 1 beta (*IL1b*) tended to be suppressed, whereas the expression of interleukin 10 (*IL10*), an anti-inflammatory cytokine, was upregulated by the salbutamol treatment (n = 4).

All data are presented as means ± standard error of the mean. Statistical comparisons were analyzed by a two-way analysis of variance with a *post hoc* Tukey's multiple comparisons test. ***P < 0.001, ****P < 0.0001, n.s.; not significant.

Supplemental Figure 2

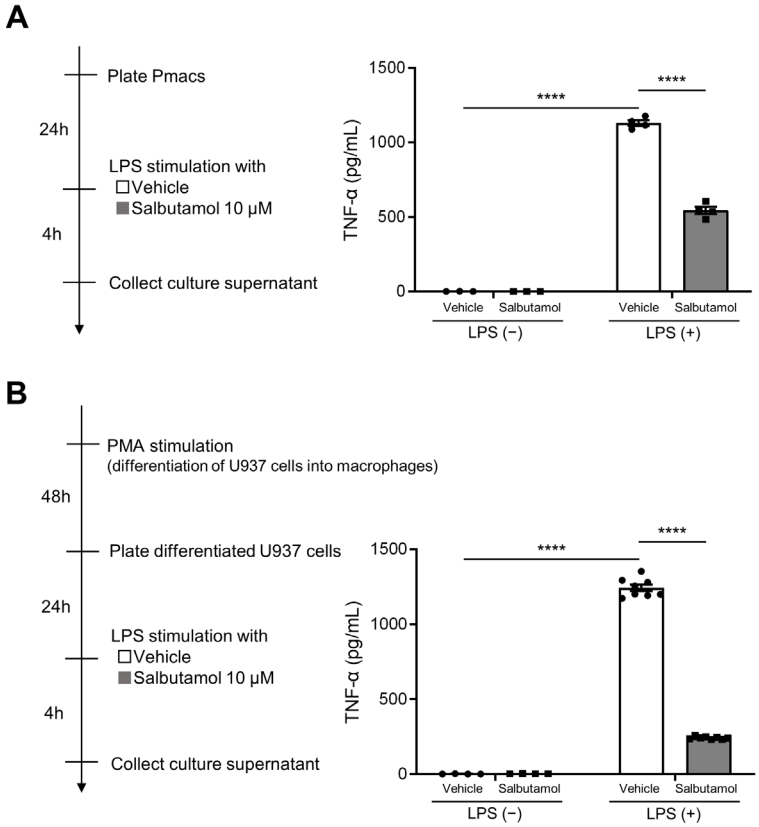

Supplemental Figure 2. The anti-inflammatory effect of β2-adrenergic receptor signaling is common in macrophages of various origins

(A) Salbutamol, a selective β2-adrenergic receptor agonist, suppressed tumor necrosis factor-α (TNF-α) induction by lipopolysaccharide (LPS) in peritoneal macrophages (Pmacs) (n = 3-4).

(B) U937 cells (human monocyte cell line) were differentiated into macrophages by phorbol 12-myristate 13-acetate (PMA) stimulation. Salbutamol suppressed TNF-α induction by LPS in human macrophages (n = 4 or 8).

All data are presented as means ± standard error of the mean. Statistical comparisons were analyzed by a two-way analysis of variance with a *post hoc* Tukey's multiple comparisons test. ****P < 0.0001.

Supplemental Figure 3

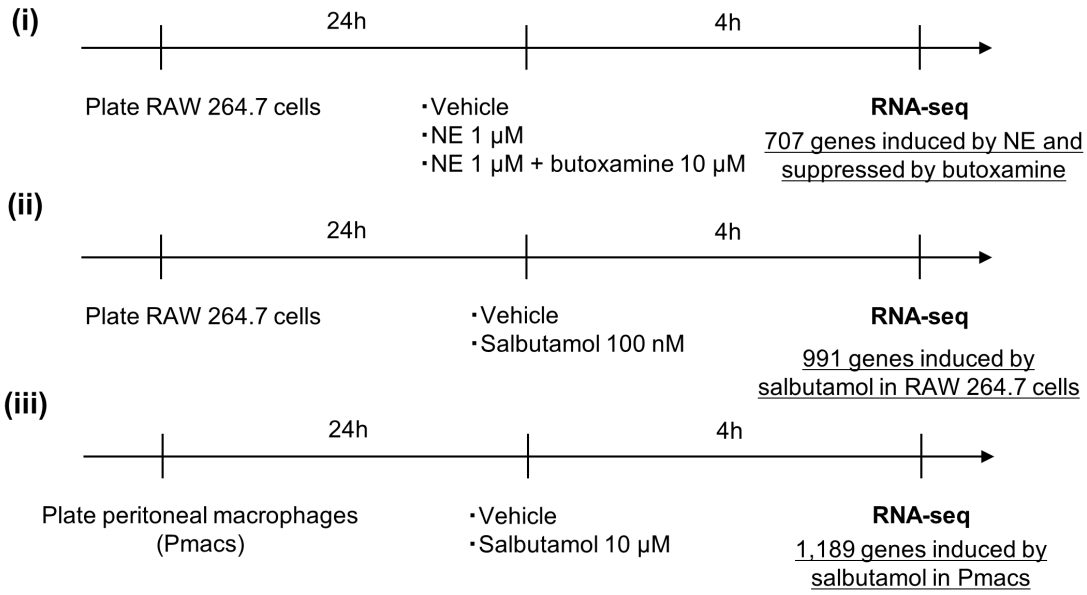

Supplemental Figure 3. The detailed protocols of RNA sequencing experiments

RNA sequencing (RNA-seq) was conducted for three different *in vitro* macrophage-models. β2-adrenergic receptor signaling-induced genes were respectively selected in each model ([i] 707 genes, [ii] 991 genes and [iii] 1,189 genes).

Supplemental Figure 4

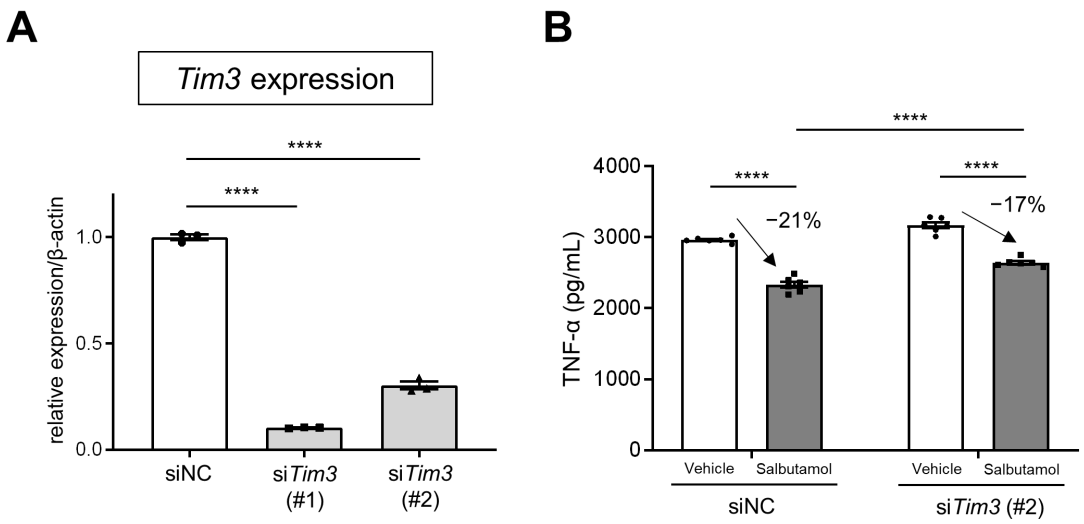

Supplemental Figure 4. The effect of T-cell immunoglobulin and mucin domain 3 knockdown using another small interfering RNA on the inflammatory response of macrophages

(A) Quantitative real-time polymerase chain reaction confirmed the efficient knockdown of T-cell immunoglobulin and mucin domain 3 (*Tim3*) by small interfering RNA (siRNA). si*Tim3* (#1) was used in Figure 2D and si*Tim3* (#2) was used in Supplemental Figure 4B (n = 3).

(B) The same experiment as Figure 2D was performed using si*Tim3* (#2) (n = 6).

All data are presented as means ± standard error of the mean. For multiplex comparisons, a one-way analysis of variance (ANOVA) (A) or two-way ANOVA (B) with a *post hoc* Tukey's multiple comparisons test was applied. ****P < 0.0001.

TNF-α, tumor necrosis factor-α.

Supplemental Figure 5

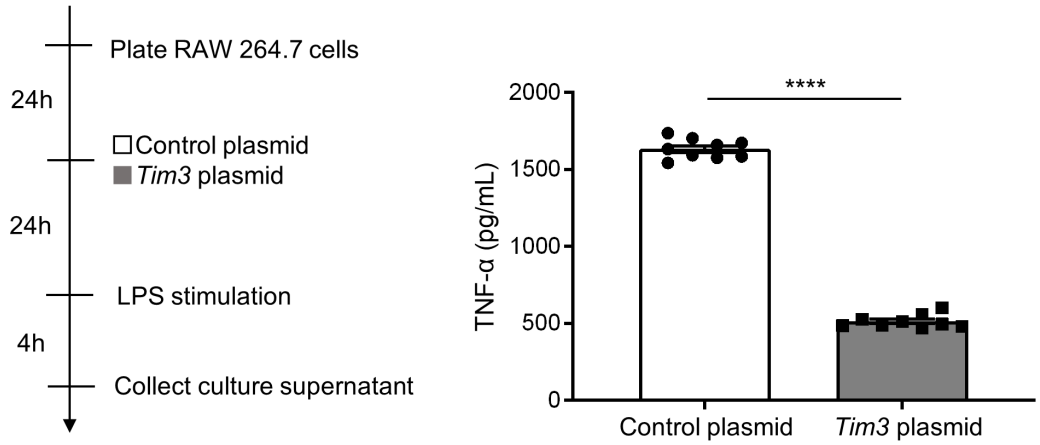

Supplemental Figure 5. The effect of T-cell immunoglobulin and mucin domain 3 overexpression on the inflammatory response of macrophages

T-cell immunoglobulin and mucin domain 3 (*Tim3*) overexpression suppressed the inflammatory response of RAW 264.7 cells (n = 9).

Data are presented as means ± standard error of the mean. The statistical comparison was analyzed by an unpaired two-tailed *t* test. ****P < 0.0001.

LPS, lipopolysaccharide; TNF-α, tumor necrosis factor-α.

Supplemental Figure 6

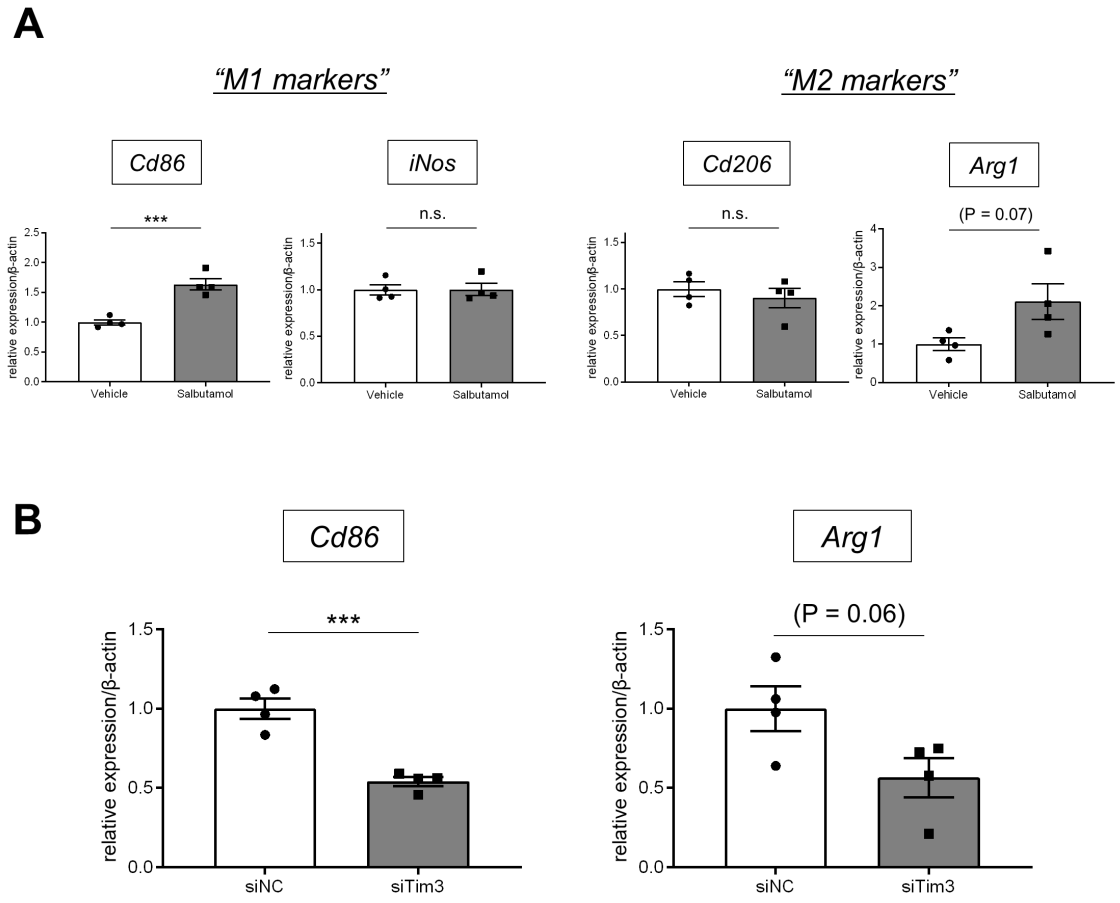

Supplemental Figure 6. The effect of β2-adrenergic receptor signaling on macrophage M1/M2 markers

β2-adrenergic receptor (Adrb2) signal-induced phenotypic alterations in macrophages could not be straightforwardly explained by the conventional M1/M2 axis because salbutamol treatment (100 nM) upregulated the expressions of M1 marker *Cd86* as well as M2 marker arginase 1 (*Arg1*). T-cell immunoglobulin and mucin domain 3 (*Tim3*) knockdown showed the opposite effects on these M1/M2 markers.

All data are presented as means ± standard error of the mean. Statistical comparisons were analyzed by an unpaired two-tailed *t* test. ***P < 0.001, n.s.; not significant.

Supplemental Figure 7

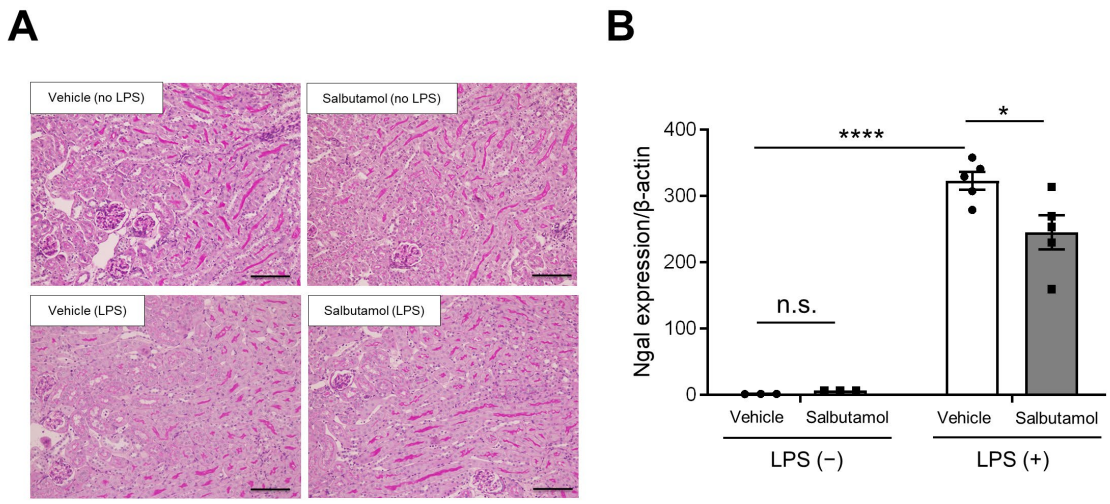

Supplemental Figure 7. Assessment of renal damage in the lipopolysaccharide-induced septic model

(A) Representative Periodic acid-Schiff staining of the renal tissues in Figure 3A is shown. Renal histological injury was not observed 4h after lipopolysaccharide (LPS) administration. Scale bar = 100 μm.

(B) The expression of neutrophil gelatinase-associated lipocalin (*Ngal*) in the renal tissues 4h after LPS administration was significantly suppressed in the salbutamol-treated group compared with vehicle-treated group (n = 3 or 5).

Data are presented as means ± standard error of the mean. The statistical comparison was analyzed by a two-way analysis of variance with a *post hoc* Tukey's multiple comparisons test. *P < 0.05, ****P < 0.0001, n.s.; not significant.

Supplemental Figure 8

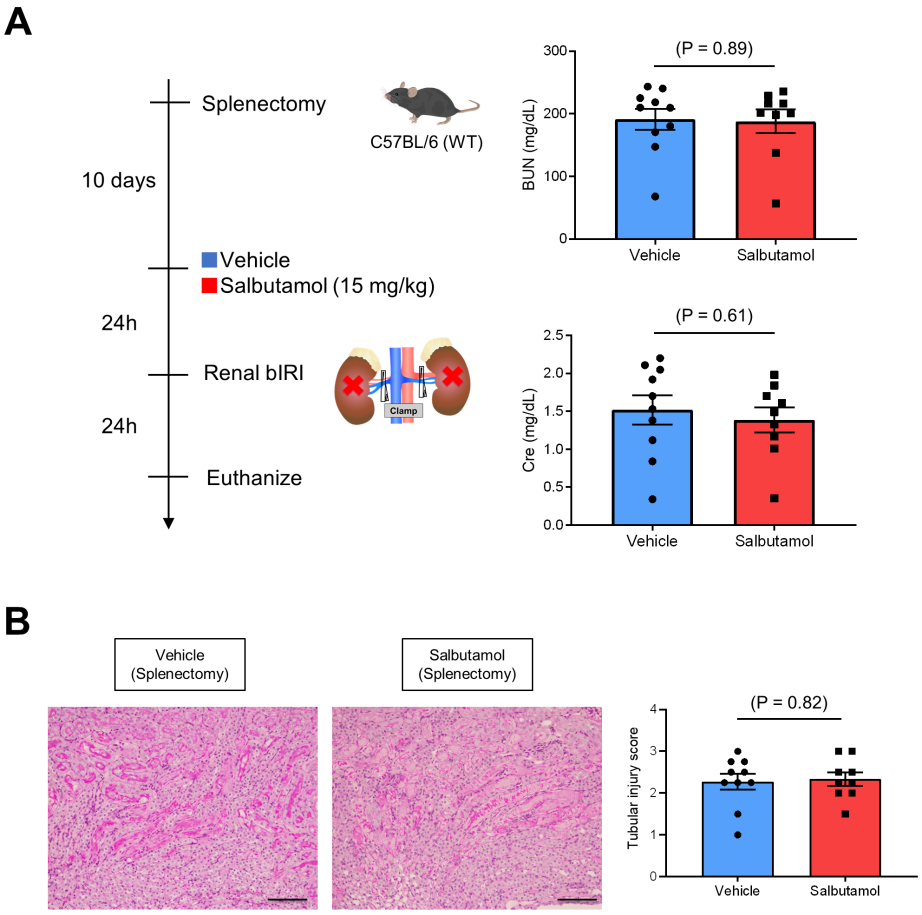

Supplemental Figure 8. Prior splenectomy abolishes the protective effect of salbutamol pretreatment against renal ischemia/reperfusion injury

(A) Vehicle or salbutamol was intraperitoneally administered to splenectomized mice 24 h before renal bilateral ischemia/reperfusion injury (bIRI). Blood and kidney samples were obtained 24 h after bIRI. The blood urea nitrogen (BUN) and plasma creatinine (Cre) levels did not differ between the vehicle and salbutamol groups (n = 9-10).

(B) Representative Periodic acid-Schiff staining of the renal outer medulla is shown on the left side (Scale bar = 100 μm). The histological tubular injury scores did not differ between groups (n = 9-10). All data are presented as means ± standard error of the mean. Statistical comparisons were analyzed by an unpaired two-tailed *t* test.

Supplemental Figure 9

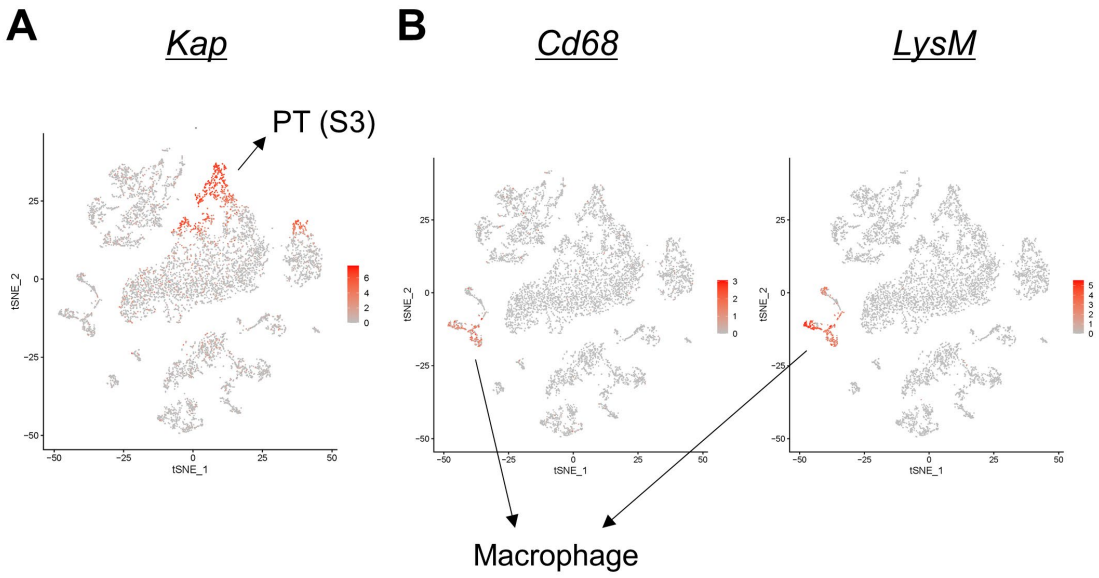

Supplemental Figure 9. Cell-type marker gene expression levels for unbiased clustering of single-cell RNA sequencing data

(A) The expression level of kidney androgen-regulated protein (*Kap*), a representative marker of proximal tubules in the S3 segment (PT [S3]), is visualized on t-distributed stochastic neighbor embedding (tSNE) plots of the single-cell RNA sequencing data in Figure 7.

(B) The expression levels of two representative macrophage markers (*Cd68* and lysozyme M [*LysM*]) are visualized on tSNE plots of the single-cell RNA sequencing data in Figure 7.

Supplemental Figure 10

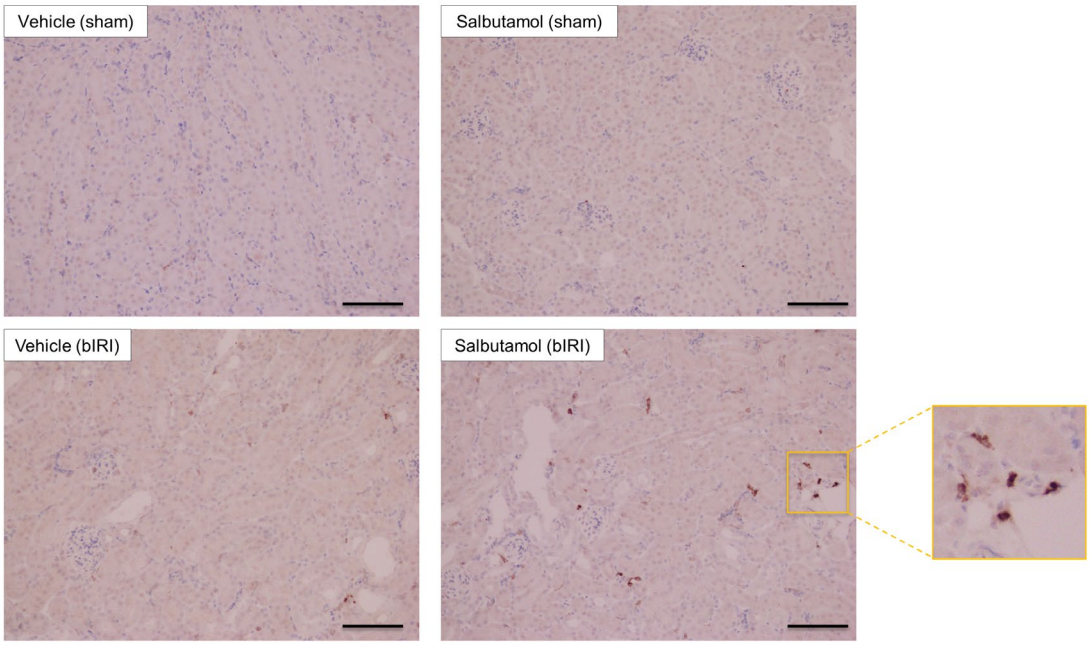

Supplemental Figure 10. Immunostaining of T-cell immunoglobulin and mucin domain 3 on renal tissues of the adoptive transfer experiment

T-cell immunoglobulin and mucin domain 3 (Tim3) immunostaining of the renal tissues in the adoptive transfer experiment (Figure 6) is shown (Scale bar = 100 μm). Tim3-positive cells were particularly accumulated in the renal tissue after renal bilateral ischemia/reperfusion injury (bIRI) followed by the adoptive transfer of salbutamol-treated macrophages.

Supplemental Figure 11

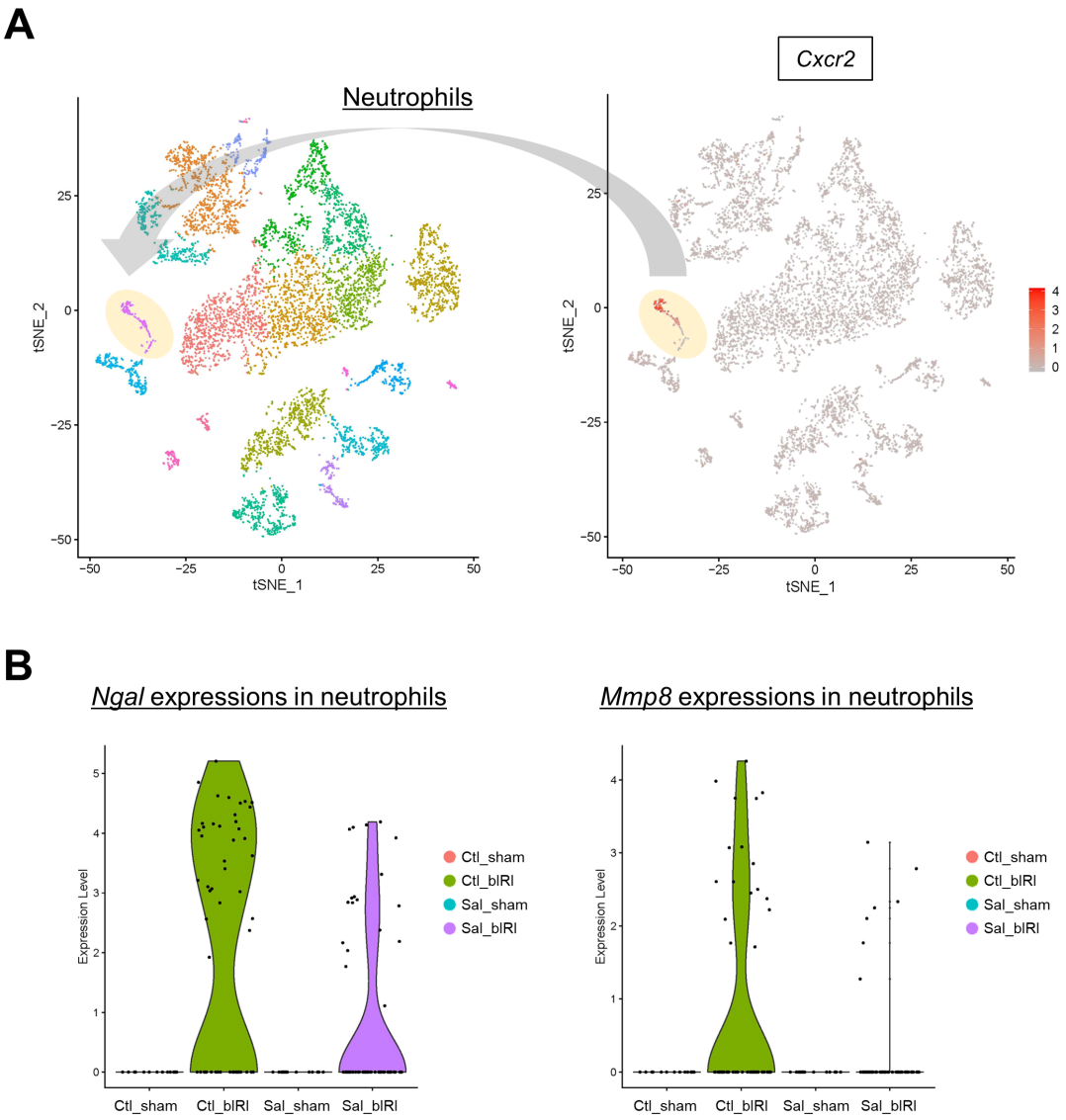

Supplemental Figure 11. Assessment of infiltrating neutrophils in the single-cell RNA sequencing data

The expression of C-X-C chemokine receptor type 2 (*Cxcr2*) identified the neutrophil cluster in the single-cell RNA sequencing data. The total number of cells in this cluster is as follows: 13 cells (Ctl_sham), 55 cells (Ctl_bIRI), 13 cells (Sal_sham), and 62 cells (Sal_bIRI). The expressions of pro-inflammatory markers such as neutrophil gelatinase-

associated lipocalin (*Ngal*) and matrix metallopeptidase 8 (*Mmp8*) in this cluster showed that the phenotype of infiltrating neutrophils might be different between Ctl_bIRI and Sal_bIRI conditions.

Ctl_sham: sham operation followed by vehicle-treated macrophage transfer, Ctl_bIRI: bilateral ischemia/reperfusion injury (bIRI) followed by vehicle-treated macrophage transfer, Sal_sham: sham operation followed by salbutamol-treated macrophage transfer, Sal_bIRI: bIRI followed by salbutamol-treated macrophage transfer.

Supplemental Figure 12

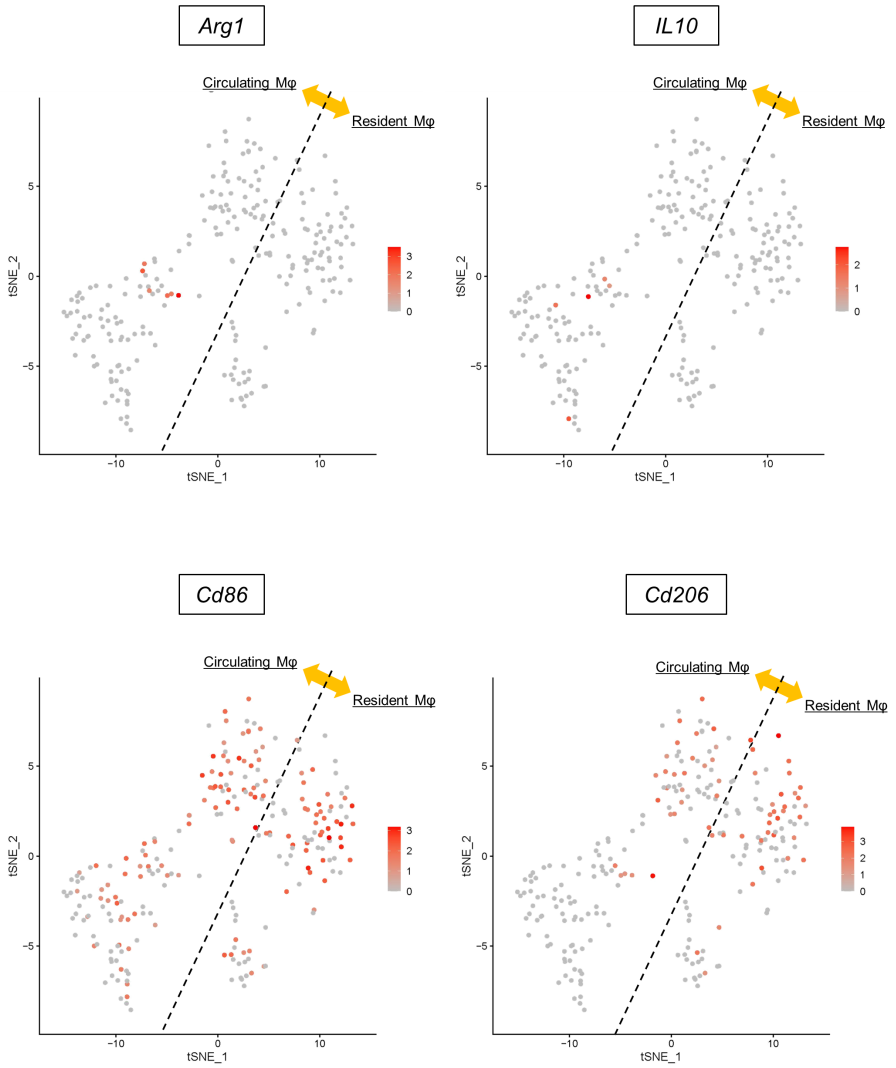

Supplemental Figure 12. M1/M2 marker gene expression levels on the macrophage sub-clustering data in the single-cell RNA sequencing

The expressions of representative M1/M2 markers on the macrophage (Mφ) cluster are shown on the t-distributed stochastic neighbor embedding (tSNE) plots. Arginase 1 (*Arg1*) or interleukin-10 (*IL10*)-positive macrophages were small in number and preferentially distributed on the left side (circulating macrophages). In contrast, *Cd86* (M1 marker) or *Cd206* (M2 marker)-positive macrophages were large in number and distributed on both sides (circulating and tissue-resident macrophages).

Supplemental Figure 13

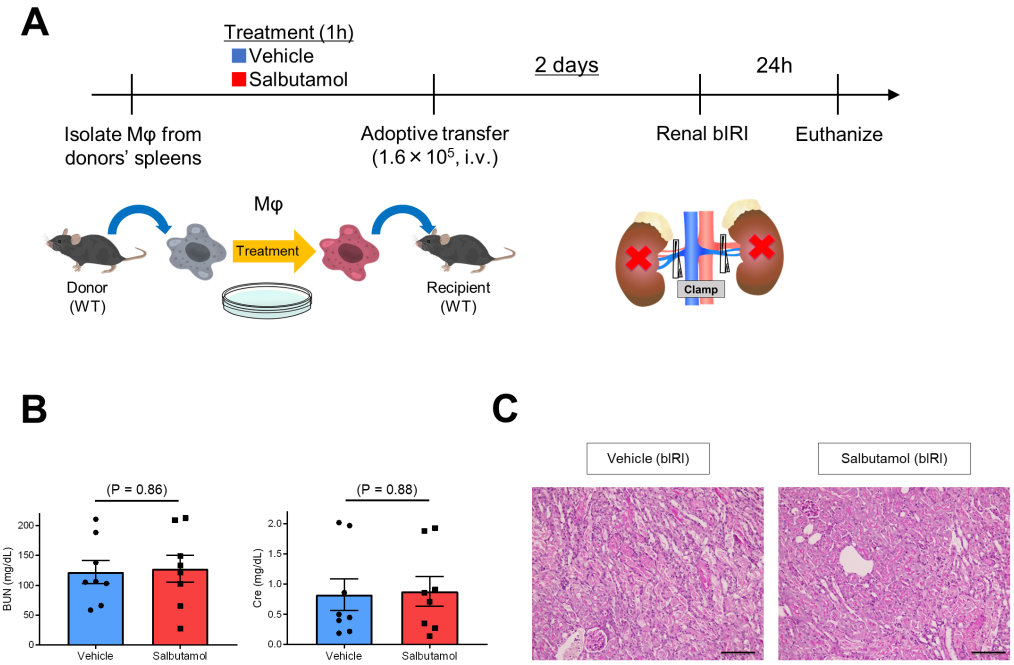

Supplemental Figure 13. The adoptive transfer of salbutamol-treated macrophages two days before renal ischemia/reperfusion injury does not provide protection

(A) The study protocol is shown. Salbutamol-treated macrophages (Mφ) from donor mice treated with salbutamol were adoptively transferred to recipient mice 2 days before bilateral ischemia/reperfusion injury (bIRI). Blood and kidney samples were obtained 24 h after bIRI.

(B) The blood urea nitrogen (BUN) and plasma creatinine (Cre) levels as well as (C) histological tubular injury did not differ between the vehicle and salbutamol groups (n = 8), suggesting that the protective effects of adoptive transfer is not maintained for two days.

All data are presented as means ± standard error of the mean. Statistical comparisons were analyzed by an unpaired two-tailed *t* test.

Supplemental Table 1. Primer sequences for the quantitative real-time polymerase chain reactions

Supplemental Table 2. A list of the marker genes of each cluster in the single-cell RNA sequencing

The marker genes sorted by average log fold-change (FC) of each cluster in the single-cell RNA sequencing are presented.

Supplemental Table 3. A list of the 37 genes commonly selected in the RNA sequencing from the three *in vitro* models

The expression of each gene is presented as log (fragments per kilobase of transcript per million mapped fragments [FPKM] + 0.001).

(Supplemental Tables were prepared as Excel files.)